Evaluation of the use of a commercially available cavity ringdown absorption spectrometer for measuring NO_2 in flight, and observations over the Mid-Atlantic States, during DISCOVER-AQ

L. C. Brent, W. J. Thorn, M. Gupta, B. Leen, J. W. Stehr, H. He, H. L. Arkinson, A. Weinheimer, C. Garland, S. E. Pusede,

Journal of Atmospheric Chemistry

ISSN 0167-7764

J Atmos Chem
DOI 10.1007/s10874-013-9265-6

Springer

J Atmos Chem
DOI 10.1007/s10874-013-9265-6

Evaluation of the use of a commercially available cavity ringdown absorption spectrometer for measuring NO_2 in flight, and observations over the Mid-Atlantic States, during DISCOVER-AQ

L. C. Brent · W. J. Thorn · M. Gupta · B. Leen · J. W. Stehr · H. He · H. L. Arkinson · A. Weinheimer · C. Garland · S. E. Pusede · P. J. Wooldridge · R. C. Cohen · R. R. Dickerson

Received: 31 March 2013 / Accepted: 23 July 2013

Abstract Real time, atmospheric NO_2 column profiles over the Mid-Atlantic states, during the July 2011 National Aeronautics and Space Administration (NASA) Deriving Information on Surface Conditions from Column and Vertically Resolved Observations to Air Quality (DISCOVER AQ) flight campaign, demonstrated that a cavity ring down spectrometer with a light emitting diode light source (LED-CRD) is a suitable technique for detecting NO_2 in the boundary layer (BL) and lower free troposphere (LFT). Results from a side-by-side flight between a NASA P3 aircraft and a University of Maryland (UMD) Cessna 402B aircraft show that NO_2 concentrations in ambient air from 0.08 nmol /mol (or ppbv) to 1.3 nmol/mol were consistent with NO_2 measurements obtained via laser induced fluorescence (LIF) and photolysis followed by NO chemiluminescence (P-CL). The current LED-CRD, commercially available by Los Gatos Research (LGR), includes the modifications added by Castellanos et al. (Rev. Sci. Instrum. 80:113107, 2009) to compensate for baseline drift and humidity through built in zeroing and drying. Because of laser instability in the initial instrument, the laser light source in the Castellanos et al. (Rev. Sci. Instrum. 80:113107, 2009) instrument has been replaced with a light emitting diode. Six independent calibrations demonstrated the instrument's linearity up through

L. C. Brent (✉) · W. J. Thorn
MML, National Institute of Standards and Technology, Gaithersburg, MD, USA
e-mail: lbrent@nist.gov

L. C. Brent · J. W. Stehr · H. He · H. L. Arkinson · R. R. Dickerson
University of Maryland, College Park, MD, USA

M. Gupta · B. Leen
Los Gatos Research, Mountain View, CA, USA

A. Weinheimer
NCAR, Boulder, CO, USA

C. Garland · S. E. Pusede · P. J. Wooldridge · R. C. Cohen
Department of Chemistry, University of California Berkeley, Berkeley, CA, USA

R. C. Cohen
Department of Earth and Planetary Science, University of California Berkeley, Berkeley, CA, USA

Published online: 25 August 2013

150 nmol/mol NO_2 and excellent stability in calibration coefficient of 1.26 (± 3.7 %). The instrument detection limit is 80 pmol/mol. Aircraft measurements over the Mid-Atlantic are included showing horizontal and vertical distributions of NO_2 during air quality episodes. During 23 research flights, NO_2 profiles were measured west and generally upwind of the Baltimore/Washington, D.C. area in the morning and east (generally downwind) of the metropolitan region in the afternoon. Column contents (surface to 2,500 m altitude) were remarkably similar ($\approx 3\times10^{15}$ molecules/cm^2) indicating that NO_2 is widely distributed over the eastern US contributing to the regional (spatial scales of approximately1000 km) nature of smog events.

Keywords Nitrogen dioxide · Cavity ringdown · Air quality · Regional smog · Flight measurements

1 Introduction

Nitrogen dioxide (NO_2), an Environmental Protection Agency (EPA) designated National Ambient Air Quality Standard (NAAQS) criteria pollutant, is known to be aggravating to the respiratory system (Schwartz and Zeger 1990; Annesi-Maesano 2006). In addition to its direct health effects, NO_2 also controls the photochemical production of Los Angeles type smog (ozone) (Jacob et al. 1996; Finlayson-Pitts and Pitts 2000) and, indirectly, the oxidizing capacity of the atmosphere. NO_x ($NO+NO_2$) released from fossil fuel combustion contributes approximately 13 % of the total global fixed nitrogen, both oxidized and reduced. These emissions contribute to the nitrogen cascade, where the same atom can cause multiple biogeochemical effects with consequences for ecosystems and human health (EPA 2006).

While the NAAQS for NO_2 is rarely, if ever, exceeded, the photochemical production of ozone in high oxides of nitrogen (NO_x) conditions leads to frequent exceedances of the 2008 8 h ozone standard set in the federal Clean Air Act. A network of ground measurement sites across the United States offers continuous 24 h monitoring, but this offers limited assessment on how the chemical and physical dynamics of the surrounding atmosphere affect concentrations at the lowest few meters of the planetary BL.

A survey of methods for measuring ambient NO_2 has been thoroughly reviewed and will not be further considered here (Fried et al. 1998; Hargrove et al. 2006; Dunlea et al. 2007; Fehsenfeld et al. 1990; Pollack et al. 2011; Dari-Salisburgo et al. 2009). The focus of the current work will be on techniques used for measuring NO_2 with respect to altitude. Collections of altitude profiles are used to gain insight into how atmospheric dynamics, both chemical and physical, affect concentrations of gas and aerosol species near the surface. Vertical column distribution provides information on BL depth, photolysis, convection and advection (Halla et al. 2011). Several methods exist for measuring NO_2 with respect to altitude. Ground based spectrometers such as NASA's Pandora collect column content with vertical resolution typically on the order of kilometers (Herman et al. 2009). Satellite spectrometers take regional snap shots of atmospheric components at regular intervals, i.e.: daily, or weekly, and are often used in global comparisons (Kim et al. 2009; Leue et al. 2001; Schaub et al. 2006). Instruments flown on aircraft are useful for measuring large latitudinal and longitudinal cross sections in addition to in situ vertical column profiles. Airborne measurements play a useful role in capturing urban versus regional distributions and the regional transport of pollutants.

Several research-grade instruments for monitoring NO_2 offer excellent sensitivity and specificity, but commercially available detectors often suffer from interferences. For example, ground monitoring stations typically rely on commercially available chemiluminescent NO_x analyzers with hot molybdenum oxide (C-Mo) converters such as the Thermo 42 series $NO/NO_2/NO_x$ analyzers. These analyzers meet EPA standards for monitoring NO_2 compliance,

but the hot MoO_x converters also convert additional oxides of nitrogen NO_z (NO_3, N_2O_5, HNO_2, HNO_3, PAN (peroxyacetylnitrate) and organo nitrates) (Fehsenfeld et al. 1987). Flight use of this instrument has been limited to estimating NO and the combination of $NO_x + NO_z$ known as NO_y (Jaeglé et al. 1998; Neuman et al. 2001; Luke et al. 1992). Two well characterized research grade instruments, frequently used in flight, are the University of California, Berkeley's (UCB), thermal dissociation laser induced fluorescence (TD-LIF) (Thornton et al. 2000; Day et al. 2002; DiCarlo et al. 2012; Bucsela et al. 2008; Wooldridge et al. 2010; Wagner et al. 2011), and the National Center for Atmospheric Research (NCAR) chemiluminescent detector with photolytic NO_2 to NO conversion (P-CL) (Ryerson et al. 2000; Emmons et al. 1997; Pollack et al. 2011; Heland et al. 2002). High correlation between these instruments and their specificity for NO_2 was demonstrated by Fuchs et al. (2010) in an atmospheric simulation chamber. Specificity for NO_2 in ambient air was demonstrated by Suzuki et al. (2011) during a ground comparison in Japan. In this comparison, LIF and P-CL measurements were in good agreement; however, measured levels of NO_2 were sometimes several nmol/mol less than levels determined with a simultaneously monitoring C-Mo instrument. The P-CL and LIF instruments have very low detection limits making them useful in low NO_x environments such as the LFT, but are not available commercially. A research grade laser-CRD for measuring NO_2 has also been used in flight. This instrument achieved a similar in-flight detection limit and compensates for drift by zeroing with gas instead of a built in chemical scrubber (Wagner et al. 2011). An advantage to these instruments, in addition to the low detection limit, is their ability to simultaneously measure multiple trace gas species. The laser-CRD is a part of a larger instrument which measures multiple oxides of nitrogen. The UCB TD-LIF uses thermal dissociation to also measure peroxynitrates (PNs), alkynitrates (ANs), and nitric acid (HNO_3). The P-CL instrument simultaneously measures O_3 and NO. The LIF and P-CL are the basis of comparison to our LED-CRD, and are described in section 3.

During July 2011, NASA conducted a portion of its DISCOVER AQ air campaign over Maryland, monitoring urban air pollution along the I-95 corridor in the Baltimore/Washington, D.C. metropolitan region. During this period, the University of Maryland complemented NASA's P3 measurements by measuring many of the same gas and aerosol species while flying a larger regional flight pattern (He et al. 2013a, b). This paper describes the evaluation of a commercially available cavity ring down NO_2 detector for airborne use. While the LED-CRD instrument detection limit and response time make it less suitable than LIF or P-CL for extreme low NO_x environments, its ease of operation and light weight make it a suitable alternative for routine ground monitoring and air quality studies aloft. The instrument was evaluated in the laboratory for sensitivity, linear dynamic range, interferences and stability. An intercomparison with established research grade instruments (LIF (UC Berkeley) and P-CL (NCAR)) was conducted at altitudes from 0.5 km to 3 km to validate LED-CRD NO_2 measurements in flight. Finally, we present upwind and downwind NO_2 profiles, during smog events in the Baltimore/Washington area, comparing regional and urban mixing ratios of the dominant ozone precursor molecule. This paper is an extension of the ground evaluation of a similar instrument performed by Castellanos et al. (2009).

2 Instrument descriptions and calibration methods

2.1 Cavity ringdown instrument description

The LED-CRD analyzer, used on the UMD Cessna 402B aircraft during the summer of 2011, was built to replace the prior laser cavity ringdown NO_2 analyzer described by Castellanos et al.

(2009). While the previous laser instrument provided accurate measurements, the laser sporadically changed frequency (i.e. "mode-hopping"), limiting the instrument's long-term sensitivity.

A theoretical and instrument description of the original CRD laser instrument manufactured by Los Gatos Research, Mountain View, CA, has been published by Castellanos et al. (2009). Briefly, as sample air is pulled through the instrument at a rate of 1.33×10^{-5} m^3/s, it is dried by Nafion® tubing with a counter flow of dry air. The flow stream is separated at a Swagelok T and controlled by a three way solenoid to go either directly to the sample cell or to first go through a chemical scrubber before entering the sample cell. The flow paths are rejoined at a solenoid fitted with Teflon® isolation valves specially designed to have zero dead volume. After the solenoid, the sample flows through a specially designed Parker VSO-EC pressure controller, to a 1.2 μm filter and into the optical cavity. The optical cavity is a 0.408 L stainless steel cylinder separating two fixed, highly reflective (99.995 %) dielectric mirrors spaced by 28.5 cm. Light enters the optical cavity perpendicular to the gas entrance through one of the mirrors. In reality, only a few micromole per mole photons of incident light is transmitted into the cavity, while the rest is reflected by the entrance mirror. Once the light is in the cavity, it is reflected back and forth many times increasing the effective path length (tc/2 L), thereby increasing sensitivity to very small NO_2 concentrations (Busch and Busch 1999). Behind the back mirror a photo multiplier tube (PMT) detector measures the light transmitted out of the cavity on each pass as a function of time. The amount of time the light spends resonating in the cavity is inversely proportional to the total loss per reflection (Lehmann et al. 2009). After the sample stream exits the cavity, a portion of it is chemically-dried (Drierite®) and used as the sheath flow for the Nafion® tubing. The sheath flow is rejoined with the exhaust gas to exit the instrument. The equations used to relate the NO_2 absorption coefficient and the rate of attenuation in the optical cavity to NO_2 concentration through the Beer-Lambert law are shown in Table 1. NO_2 concentrations are determined by the amount of time it takes the light to decay as measured by the photomultiplier tube (PMT). In principle, cavity ringdown should provide an absolute measure of concentration because the technique is dependent

Table 1 A table of equations relating cavity length, intensity and the molecular cross section to the Beer-Lambert law so that the NO_2 concentration can be derived from the difference between the ringdown decay rate and background the background decay rate

tc/2L=path length
(1-R)=loss per reflection
$I(t)=I_o \exp(-\sigma LN)$
$I(t)=i_o \exp[-(1-R)tc/L]$
$\alpha=(1/c\sigma)(1/\tau - 1/\tau_o)=\sigma N$

t	Time
c	Speed of light
R	Reflectivity
I_t	Transmitted intensity
I_o	Incident intensity
σ	Wavelength specific cross section of absorbing species
L	Length of cavity
N	Number density of absorbing species in cm^{-3}
α	Wavelength dependent absorption coefficient

upon well-defined physical parameters such as the wavelength dependent molecular cross section, path length, temperature, and pressure of the optical cavity.

The instrument highlighted in this paper is a modification of the original laser CRD (Castellanos et al. 2009) with the most significant difference being that the laser light source was replaced by a light emitting diode (LED) (355 mW, Lumileds, Prolight). The LED emission spectrum is 397 to 412 nm with peak emission at 408 nm. The light is filtered through a 10 nm wide spectral bandpass filter centered at 405 nm. While, in an empty cavity, the ring-down transients are slightly multi-exponential, the mirror reflectivity is flat across this spectral range. In effect the LED is not broad band compared to the mirror band so the signal can be treated as a single exponential. If the ring-down transient were strongly multi-exponential, the calibration curve would deviate from first order with increasing NO_2. The LED is temperature stabilized through mounting on a thermoelectrically cooled plate and is current modulated with a fall time of 300 ns and a pulse modulation rate of 5 kHz. Ringdown events are collected using a data acquisition (DAQ) card operating at 1.25 MHz. The convolved LED-PMT-DAQ 1/e response time is 660 ns. Individual ringdowns are boxcar averaged in groups of 1,000 and the resulting average trace is fit to a decaying single exponential using a non-linear least squares fit.

The instrument includes a manufacturer installed 1.2 μm filter positioned between the pressure controller and the inlet to the optical cavity, but because submicrometer environmental aerosols can interfere with gas measurements, an additional 0.1 μm filter has been placed at the instrument inlet. The period over which the filters should be changed is still a subject of study. The internal cavity pressure is maintained at 40,263 Pa, increased from 22,665 Pa in the laser instrument. The stainless steel optical cavity pressure and temperature are monitored to convert the NO_2 number concentration to a mixing ratio. While the optical cavity pressure in this instrument is increased by 30,931 Pa, the sample residence time, defined as volume / flow, is the same because the pumping rate was increased from 8.3×10^{-6} m^3/s (0.56 slpm) to 1.33×10^{-5} m^3/s (0.8 slpm).

2.2 Calibration procedures

2.2.1 Standard addition

Standard dilution at the National Institute of Standards and Technology (NIST) was a multistep process beginning with the preparation and concentration determination of a nitrogen dioxide working standard, prior to serial dilution and measurements. In our calibration process, a Thermo 42C chemiluminescence detector with a stainless steel thermal converter (C-SS) operating at greater than 600 °C was used to verify a NO_2 working standard. While chemiluminescence instruments employing thermal conversion from NO_y to NO are known to lack NO_2 specificity, Fried et al. (1998), has determined their suitability for this laboratory work through independent comparison to NO_2 specific techniques, tunable diode laser spectroscopy and Fourier transform infrared spectroscopy. In Fried et al. work, the NO_2 values agreed with the chemiluminescence measurements when a Nylon® prefilter for removing the primary impurity, HNO_3, was placed at the inlet, prior to thermal conversion. In our work, NO_x to NO thermal conversion efficiency approaching 100 % was achieved using a pre converter (Stainless Steel, ~700 °C, 101 kPa) in series with NIST's Thermo Model 42C ambient level instrument which is equipped with a similar thermal converter (stainless steel, 635 °C, 10 kPa). The chemiluminescence detector was calibrated indirectly for NO_2 by quantitatively comparing the thermal dissociation of NO_2 to NO to gravimetric standards containing NO in N_2.

Preparation of the NO_2 standard was as follows. Reagent grade nitrogen dioxide is diluted with nitrogen to achieve the desired concentration of NO_2 in nitrogen. A cylinder containing

2.3 kg of ultra-high purity nitrogen dioxide (99.5 % minimum purity), was obtained from Matheson Trigas in December, 2002. In 2009 the NO_2 standard was analyzed and it was found that the purity had degraded to < 98 % of the original concentration. Reaction of the NO_2 with the DOT 3AA specification steel cylinder inner walls evidently produced HNO_3 and H_2O contamination. The reagent NO_2 was distilled three times and passed through a P_2O_5 drier to remove water and then passed through a Nylon® membrane filter to remove nitric acid. The final purity was determined to be 99.0 % after clean up.

Reagent NO_2 was serially diluted with nitrogen in steps to 4000 μmol/mol>500 μmol/mol> 100 μmol/mol>10 μmol/mol. The NO_x concentration was determined by direct measurement against a NO in N_2 standard referencing material (SRM) or NIST gravimetric primary standard at similar NO_2 concentrations of 4000, 500, 100, 10 μmol/mol. NO_2 values were determined by measurement of NO_x before and after a 1 μm Nylon® membrane filter which trapped HNO_3. The stability of six working standards containing≈10 μmol/mol NO_2 in N_2 was evaluated over a period of 5 years. After 2 years, levels of NO_2 in five of the six working standards stabilized after an initial decrease in NO_2. The sixth mixture continues to drop for reasons unknown (Thorn et al. 2010). The working standard was prepared from this batch of NO_2 standards.

The Luxfer DOT 3AL 6 L aluminum cylinders used at NIST for all NO and NO_2 standards have an extremely smooth inner wall surface resulting from the high pressure extrusion process used in their manufacture. The surface is aluminum oxide (Al_2O_3), an amphoteric oxide, which acts as a weak base in the presence of a strong acid like HNO_3. To produce stable concentrations of NO in N_2 below 10 μmol/mol it is necessary to titrate the aluminum oxide surface with nitric acid which is done by exposing the walls to 1000 μmol/mol NO_2 in N_2. NO_2 reacts with the ubiquitously adsorbed water forming adsorbed $HNO_3 + HNO_2$. After titrating the cylinder wall, excess $HNO_3 + HNO_2$ will desorb from the wall into the cylinder gas mixture. Excess NO_2 treatment gas is removed from the cylinder through several purges with 99.999 % nitrogen, (purity achieved with Airgas trademarked built in purity technology (BIP®)) followed by vacuum elimination. The cylinder is rendered ready for maintaining NO stability at low concentrations. All NIST NO primary standard mixtures are blended gravimetrically using BIP® nitrogen to remove trace oxygen (~1 μmol/mol) from nitrogen.

After verification of the C-SS response to NO and verification of complete NO_2 to NO conversion, the UMD NO_2 working standard was evaluated. Calibration of the LED-CRD absorption spectrometer was completed by comparing readings of NO_2 standard serial dilutions to flow dilution calculations and to values obtained on the Thermo 42C. The least squares fit between the Thermo 42C measured NO_2 concentrations and the flow dilution calculations had a slope of 1.01 and correlation coefficient of >0.999.

2.2.2 Gas phase titration

During gas phase titration (GPT), NO_2 was produced by reaction of NO with O_3. The GPTs conducted at both NIST and UMD used a Thermo 49PS as the ozone source; NO was from either a NIST SRM or a NIST traceable commercial standard. Both Thermo 49PSs were calibrated against the NIST ozone standard reference photometer before use and found to have slopes of 0.9981 and 1.001, respectively. GPT calibrations at NIST and at the Beltsville Agricultural field site were conducted in excess NO. The UMD GPT was conducted in excess ozone.

At UMD the same GPT procedure as published in Castellanos et al. 2009 was used. Before calibration, a commercial Scott Marin NO in N_2 standard was ratioed against the SRM 2627a and determined to be 4.868 nmol/mol (+/− 1 %) NO / 4.818 nmol/mol (+/− 1 %) NO_x. During this procedure, NO was diluted with air (9.1 nmol/mol to 96 nmol/mol) and mixed with

300 nmol/mol O_3 in air in a 3 L round bottom flask. The amount of NO_2 produced was compared to simultaneous LED-CRD absorption readings on a laser-CRD NO_2 instrument. The laser-CRD instrument (Castellanos et al. 2009) had undergone the same standard dilution calibration at NIST as described above. The slope and correlation coefficient of the laser instrument to the NIST CL-thermal converter was 1.00 and 0.999, respectively.

At NIST the GPT NO_2 concentrations were verified by measurements of ozone loss, and by measuring the amount of NO loss on a Thermo 42 C NO-NO_2-NO_x detector. At the field site, NO_2 production was verified by O_3 loss on NOAA's 3-channel chemiluminescence detector with photolytic NO_2 to NO conversion using a blue light converter (λ_{max} 395±5) lamp. NO_2 was measured as the difference between NO and NO_x (Luke et al. 2007).

2.3 Instruments used for flight intercomparison

2.3.1 Photolysis followed by chemiluminescence (P-CL)

The NCAR four channel chemiluminescent instrument operated on the P3 measures NO, NO_2, NO_y, and O_3. A description of this instrument can be found at http://discover-aq.larc.nasa.gov/pdf/2010STM/Weinheimer20101005_DISCOVERAQ_AJW.pdf (last accessed 24 June 2013). This instrument measures NO_2 with a process similar to that used by the Thermo 42C described above. As the combined oxides of nitrogen enter the instrument, NO is quantified directly after second order reaction with ozone (generated inside the instrument), to produce NO_2. NO_2 chemiluminescence is proportional to the original NO concentration. NO_2 and NO_y are converted to NO and measured as an increase in chemiluminescent signal above ambient NO. Like the Thermo 42C, the total NO_y species are converted to NO ($NO_y + M \rightarrow NO + M\text{-}O_y$) with a heated metal catalyst. This analyzer distinguishes itself from the Thermo 42C by selectively measuring NO_2 on a separate channel. NO_2 is photodissociated to NO by illumination from 400 nm LEDs, with a conversion efficiency near 90 % that is measured several times during a flight by calibrating with a known flow of NO_2. The NO_2 1 s, 2σ detection limit is 60 pmol/mol with an overall uncertainty of 10 to 15 %. The instrument response time for NO_2 measurements is ≈ 3 s.

2.3.2 Laser induced fluorescence

The TD-LIF instrument, operated by the University of California Berkeley on the P3 aircraft, uses LIF to directly detect NO_2. A custom built, Nd:YAG laser pumps a tunable dye laser (λ=585 nm), which is used to excite a narrow rovibronic feature unique to NO_2. The laser light is focused into two multipass cells and red shifted fluorescent photons at wavelengths longer than 700 nm are counted. A background signal is referenced by shifting the laser frequency off the NO_2 feature. Instrument zeroing is performed by over pressurizing the inlet with zero air. The NO_2 slope has 5 % uncertainty and the 1 s, 2σ detection limit is 30 pmol/mol. The instrument response time is ≤ 1 s. For a complete description of LIF see Thornton et al. (2000). Three additional channels sample air through ovens held at temperatures 200 °C, 400 °C, and 600 °C in order to thermally dissociate PNs, ANs, and HNO_3, respectively, to NO_2 plus a companion radical. PNs, ANs, and HNO_3 are then measured by quantifying the difference between adjacent channels (i.e. ANs are equal to the difference between the 200 and 400 °C channels). The accuracy for PNs, ANs, and HNO_3 also includes terms for transmission efficiency through the sampling inlet and the completeness of thermal dissociation and is estimated to be 15 %. A complete description of this process is available in Day et al. (2002). See Table 2 for a summary of aircrafts, organizations, uncertainties and measurement times respective to each measurement technique.

Table 2 The instrument uncertainty and averaging time for data presented in this paper

Plane	Technique	Organization	Uncertainty	Avg time
Cessna 402 B	CRD	UMD	5 %	10 s
P3	Chemi	NCAR	30 %	10 s
P3	LIF	UC Berkeley	5 %	10 s

3 Aircraft and flight patterns

The UMD aircraft is a Cessna 402B, an unpressurized plane whose flight operations are limited to an altitude of 3 km. The NASA P3 aircraft is a pressurized four engine turboprop that can fly as high as 9 km, but only flew to 5 km for DISCOVER AQ. Both aircraft were outfitted with a series of gas and aerosol instruments, but comparisons in this paper, are limited to NO_2 up to 3 km.

3.1 Side-by-side flight plan

The Cessna 402B and the NASA P3 met at 2.6 km due south of the Massey Aerodome Airport, Massey, MD and flew S/SE in a near wing tip to wing tip, side-by-side configuration for 16 min. The 2.6 km transect ended over Selbyville, DE, where the two aircraft then spiraled downward to 0.61 km over the Delaware / Maryland border. At 0.61 km, the downward spiraling stopped and the two planes flew a side by side transect for 12 min in a W/NW direction ending near Ridgley, MD. The cavity ringdown NO_2 instrument was zeroed for 3 min at 2.6 km before the comparison began and zeroed again at 0.61 km for ten minutes after the P3 departed. The side by side flight path is shown in yellow on Fig. 1. The flight speed ranged from 50 to 110 m/s. With a 10 s instrument averaging time, the horizontal measurement resolution was 540 to 1,080 m.

3.2 Westerly transport flight plan

The UMD westerly transport flights are designed to capture transport of pollutants across the Maryland ozone nonattainment region. AM flights include spirals in rural areas of western Maryland and Virginia, generally upwind of the nonattainment region. Afternoon flights include spirals performed over rural county airports downwind of the Baltimore / Washington region, and in the nonattainment region. Information gathered from these flights is used to gain insight into the local versus regional nature of the Maryland nonattainment problem. In Fig. 1, the UMD AM/Upwind flight plan is shown in red, the UMD PM/Downwind flight plan is shown in blue, and the NASA P3 urban corridor flight path is shown in green. The AM flights flew between 1300 to 1630 h UTC (coordinated universal time) and the PM flights ran from 1730 h to 2030 h UTC. Solar noon ranged from 1607 to 1614 UTC, from the first flight day, June 8th to the last day, July 29th. A summary of spiral direction with respect spiral location is provided in Table 3. The P3 generally began reporting measurements around 1400 UTC and the flights lasted approximately 7 h flying 18 profiles per flight.

4 Results and discussion

4.1 Calibration and stability

The NO_2 LED-CRD analyzer was calibrated at NIST by standard dilution resulting in a calibration curve of $NO_{2(LED\text{-}CRD)(nmol/mol)}=(1.29\pm0.004) * NO_{2ref(nmol/mol)} -$

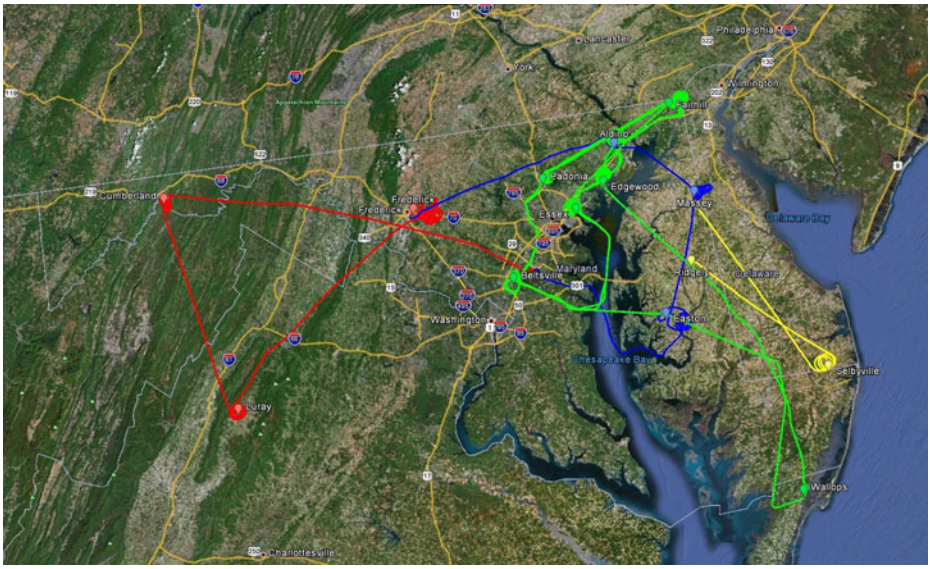

Fig. 1 The UMD Cessna upwind/rural/AM (1300–1630 UTC) flight path is shown in *red*, the Cessna downwind/rural/PM (1730–2030 UTC) flight path is shown in *blue*, and the NASA P3 flight path is shown in *green* (usually ~1400–2000 UTC). The Cessna / P3 side by side flight path flown over rural areas of Maryland and Delaware is shown in *yellow*. The planes were a few meters apart during the constant altitude phases. Local solar time is approximately 4 h earlier than UTC

($1.14_{(nmol/mol)}$±0.22). Four additional verifications of the calibration coefficient were conducted between May and September, 2011. Three gas phase titrations (GPT) were performed, each at a different location (NIST, the Beltsville, MD field site and at the University of Maryland), and another standard dilution was performed at NIST. The average slope of the five calibrations is 1.26 (uncertainty 3.7 %). The calibration curves and correlation coefficients for each calibration are shown in Table 4. The linearity of the five curves is shown in Fig. 2. The calibration curves overlap particularly well in the range relevant to atmospheric concentrations (a few pmol/mol to approximately 30 nmol/mol to 50 nmol/mol).

Table 3 The AM and PM Cessna regional flight path consisted of 3 spirals over airports in western Maryland and Virgina and upwind of the metropolitan nonattainment area and 3 spirals over Maryland downwind of the nonattainment area

AM / upwind flight plan	Coordinates	AM spiral direction	PM / downwind flight plan	Coordinates	PM spiral direction
Cumberland, MD (CBE)	39.61500	↑	Aldino, MD (0W3)	39.56683	↓
	−78.76222			−76.20240	
Lurray, VA (W45)	38.66705	↑	Massey Aerodome, MD (MD1)	39.30458	↑
	−78.50058			−75.79468	
Frederick, MD (FDK)	39.41666	↓	Easton, MD (ESN)	38.802776	↓
	−77.41666			−76.06778	

The only spiral in our flight plan also flown by the P3 was the Aldino spiral (0W3). The Cessna flew a downward spiral while the P3 flew an upward spiral. The Cessna was in close proximity to the P3 during four of the Aldino spirals (July 10, 21, 23, and 29)

Table 4 Calibration curve data

Location	Month	Technique	Reference	Range (nmol/mol NO_2)	Calibration curve
NIST	May	Standard dilution	Flow control calculation	3.5 to 99.1	Y=1.29X – 1.14
NIST	June	GPT	Δ O_3	10.5 to 96.1	Y=1.26X – 0.39
NIST	June	GPT	Δ NO	10.5 to 96.1	Y=1.29X – 1.60
UMD	June	GPT	Laser CRD	9.1 to 96	Y=1.32X – 0.45
Beltsville	August	GPT	Δ O_3	33 to 156	Y=1.19X – 0.06
NIST	September	Standard dilution	Flow control calculation	0.8 to 35.6	Y=1.23X – 0.18

To validate the LED-CRD, the instrument was calibrated at NIST through standard dilution. The calibration coefficient was verified four times, at three locations, by two different techniques. R^2 was always greater than 0.99

Additionally, a month long comparison to the same NOAA chemiluminescence detector (P-CL, NOAA) using photolytic conversion, as described by Castellanos et al. was conducted. The ground based instrument intercomparison was conducted at the Beltsville, MD, U.S. Department of Agriculture Beltsville, Agricultural Research Center field site, in a climate controlled trailer. The field site continuous monitoring, month long comparison, between the LED-CRD and the P-CL, NOAA measurements yielded a line of $NO_{2\ (LED\text{-}CRD)}=(0.98\pm0.001)*P\text{-}CL_{NOAA} - (0.40\pm0.006)$, and correlation coefficient of $R^2=0.97$. The gas phase titration conducted at the field site, resulted in a curve of $NO_{2(LED\text{-}CRD)}=(1.19\pm0.019)*NO_{2(\Delta O3)} - (0.06\pm1.88)$, $R^2=1.00$.

The comparison between the original laser-CRD and the new LED-CRD for the GPT performed at UMD resulted in a calibration curve of $NO_{2(LED\text{-}CRD)}=1.32*NO_{2(Laser\text{-}CRD)} - 0.45$. The original NO_2 cross section used in the LED instrument was approximated from first principles. Because of complicated interplay between the LED spectrum and NO_2 absorption, the first principle estimate required a 30 % adjustment.

4.2 Detection limit, residence and response time

As is typical for CRDS instruments shot noise dominated the noise of the laser instrument 3 σ detection limit (Lehmann et al. 2009). From a reading of zero air, the laser instrument 3 σ

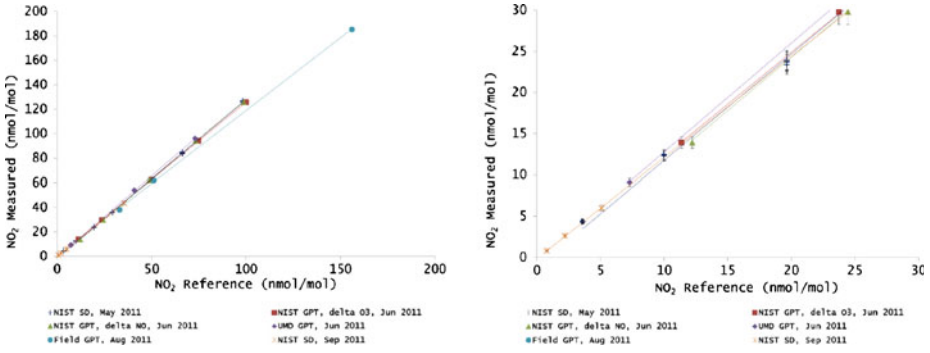

Fig. 2 Results from the NIST calibration and periodic calibration coefficient verification is presented in Fig. 2a. The average calibration factor is 1.26 (± 3.7 %). The curves overlap particularly well up between 0 and 30 nmol/mol (Fig. 2b.) the concentration range relevant to atmospheric measurements

detection limit was estimated as 0.2 nmol/mol integrated over 10 s and 0.06 nmol/mol integrated over 60 s. In the LED instrument, random baseline drift is the dominant source of noise, so even though the detection limit with a 10 s integration time is reduced to 80 pmol/mol, longer integration times do not give the benefit of lower detection limits. Hence, the 3 σ detection limit, for a 60 s integration time, remains at 80 pmol/mol. Furthermore, because the drift creates excess baseline variability, the instrument should be zeroed frequently. During the side by side flight, a linear interpolation of zero data, 60 s, before and after the side by side comparison, also resulted in an 80 pmol/mol NO_2 in ambient air 3 σ detection limit.

Quick instrument response time decreases the likelihood of measurement bias during calibration and rapidly changing environments. The EPA Operators Guide to eliminating bias in continuous emissions systems refers to instrument response time as the seconds required to reach 95 % of the asymptotic value after a change in concentration, equivalent to three e-folding time constants for a system with first order response (United States Environmental Protection Agency et al. 1994). Similar to the laser-CRD, a first order response to a step change in concentration was observed for the LED-CRD but a faster pump reduced the time to reach 95 % of the new signal ($\ln(0.05)/-k=\tau$) to 3.7 s (from 18 s). The residence time for gas in the optical cavity (time=flow/volume) is 11 s.

4.3 NASA P3 and Cessna 402 side by side flight data comparison

During a side by side flight flown over eastern Maryland and Delaware the University of Maryland, cavity ringdown NO_2 measurements were compared to two separate, NO_2 measurement techniques on the NASA P3. Figure 3 is a plot of the side by side trace gas data. Figure 3a, shows that the LED-CRD compared well to the NCAR P-CL and the UCB LIF research instruments for mixing ratios ranging from the LED-CRD detection limit (80 pmol/mol) to 1.3 nmol/mol NO_2 in ambient air.

The side by side flight experiment consisted of three phases, a 14 min, 2.6 km transect, a 14 min descending spiral from 2.6 km to 1.6 km, and a 14 min 0.6 km transect. During the 2.6 km transect, the P-CL and LIF each measured average concentrations of 0.06 (+/− 16 %) nmol/mol while the LED-CRD average NO_2 was 0.08 (+/− 100 %) nmol/mol NO_2 in air (i.e. at the detection limit). The P-CL and LIF LFT NO_2 concentrations measured here are similar to those reported in Blonde et al.'s 2007 globally averaged GOME result. A majority of NO_2 concentrations at this altitude were found to routinely fall near or below the LED-CRD detection limit. During the descending spiral, tropospheric NO_2 concentrations increase into the 3 σ detection range, near 1.6 km, thereby increasing the confidence in the reported values (Skoog et al. 1998). The peak maximum observed by all three instruments, near the beginning of the low altitude, 0.6 km transect, at 19:09 UTC, corresponds to emissions from the Indian River Generating Station according to a back trajectory of winds performed in HYSPLIT (http://ready.arl.noaa.gov/HYSPLIT_traj.php). This is an active, coal-fired electrical generating facility located at the confluence of the Indian River and Island Creek in Sussex County Delaware. CO, SO_2, NO, and NO_y also showed corresponding peaks and this data is available to the public at http://www-air.larc.nasa.gov/missions/discover-aq/P3B-extract.html. See Fig. 3b. At 1.30 nmol/mol NO_2 in air, the plume concentration exceeds both the limit of detection and limit of quantitation (10 σ baseline noise) and the measurement uncertainty fell to 5.1 %. Because the NIST standard addition calibration uncertainty is estimated to be 1 %, baseline drift drives the measurement uncertainty. The peak base is 210 s wide which corresponds to a horizontal distance of 19 km.

Correlation of the 10 s averaged LED-CRD data to the P-CL and LIF 10 s averaged data is shown in Fig. 4a and b. Plots of the LED-CRD data to the P-CL and LED-CRD vs. LIF have slopes 1.07 and 1.08, respectively, with R^2 values of 0.932 and 0.899 respectively. Agreement

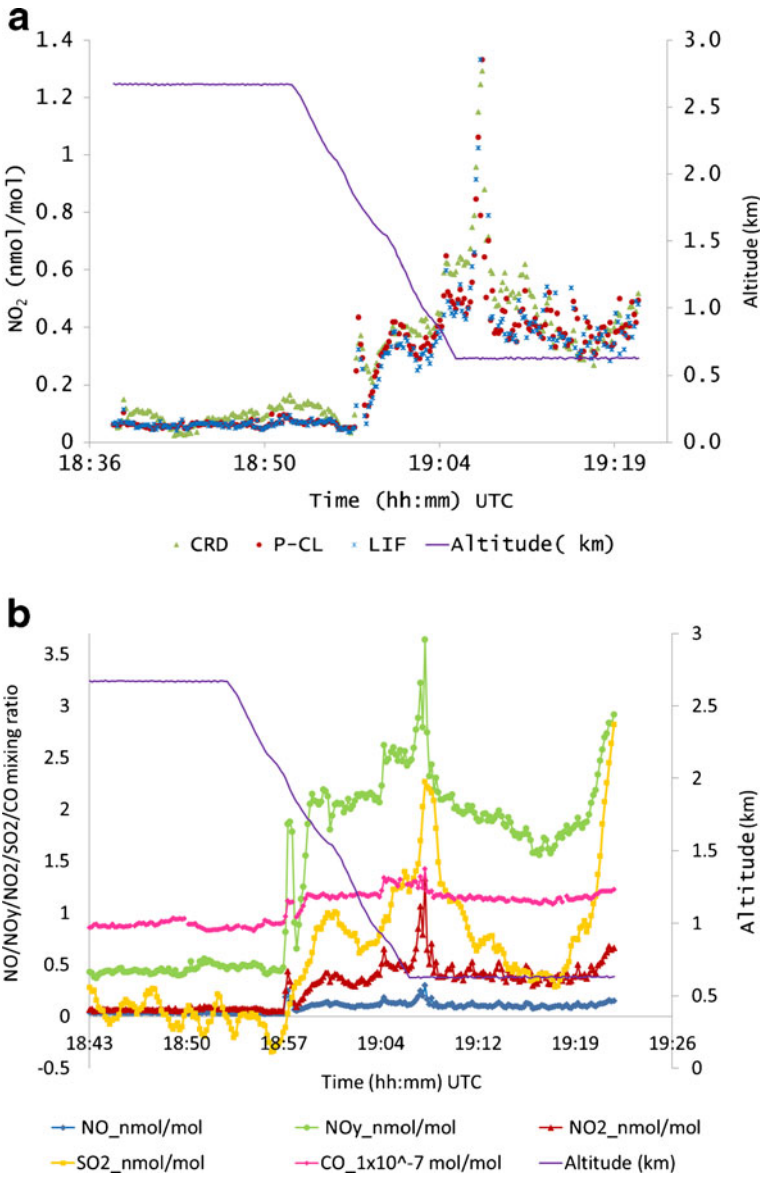

Fig. 3 **a** Time series of NO_2 measured from 1836 to 1920 EDT on 27 July 2012. Signals from each instrument are averaged to 10 s intervals. LIF and P-CL were aboard the NASA P3 and the CRD was aboard the UMD Cessna 402B. **b** Simultaneous increases in other trace gases were observed with the increase in NO_2

between LIF versus P-CL has a slope of 0.94 and R^2 of 0.939. Table 5 extends the comparison to include 1 s and 60 s averaged data. Improved temporal resolution and less propagated error generated from data binning shows correlation coefficients between CRD and the other NO_2 measurements closer to unity. This side by side flight data demonstrates that the commercial Los Gatos cavity ring down NO_2 gas analyzer is suitable for pollution studies in the BL and LFT.

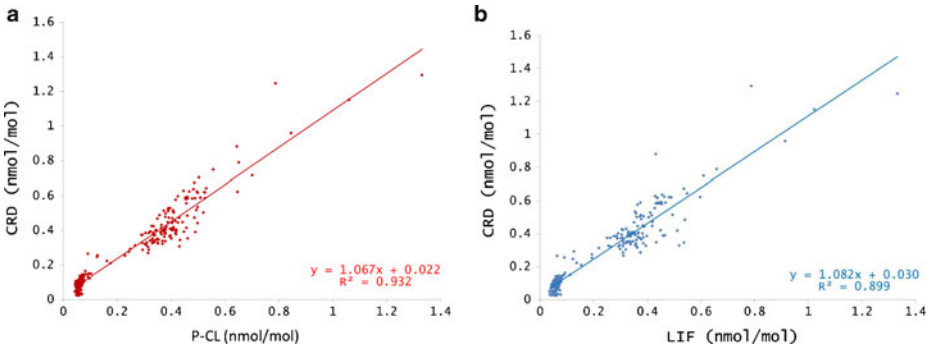

Fig. 4 **a** The UMD cavity ringdown NO_2 measurements collected on the Cessna 402B are plotted against the National Center for Atmospheric research Chemiluminescent NO_2 measurement (with a 400 nm LED for NO_2 to NO conversion), collected on the NASA P3. **b** The UMD cavity ringdown NO_2 measurements are plotted against the University of California Berkeley LIF NO_2 measurements collected on the NASA P3. The scatter plot of 10 s averaged data show a near 1:1 correlation

4.4 Summary of summer 2011 NO_2 measurements

4.4.1 NO_2 column content

In the eastern U.S., the natural abundance of hydrocarbons makes NO_2 the critical ozone precursor. Once NO_2 is formed, its complicated lifetime is dictated by a series of pathways such as sequestration into longer lived reservoir species PAN (peroxyacetyl nitrate) and alkylnitrates, removal through photolytic dissociation to nitric oxide and odd oxygen allowing for ozone formation, and/or wet or dry deposition after reaction with OH to produce nitric acid. Knowledge of the vertical distribution and characterizing the abundance in and above the BL is necessary for successful predictive modeling of ground level ozone concentrations (Logan 1989; Napelenok et al. 2008). Percentile binning of the 2011 summertime data, Fig. 5, show that the BL and LFT can be stratified into three general horizontal cross sections. Looking at the median value, between the ground and 1.3 km, NO_2 has the most variation due to BL fine structure resulting from point source influence. For instance, the highest summer time flight NO_2 measurements were of ship plumes during low level flights over the Chesapeake Bay. At

Table 5 A comparison between the 1 s, 10 s, and 60 s scatter plots for NO_2 measured by three instruments during the 27 July 2011 side by side flight

Technique	Slope (m)	e_m	Intercept (b)	e_b	R^2	Avg time (s)
CRD vs P-CL	1.009	0.008	0.041	0.003	0.844	1
CRD vs LIF	0.950	0.011	0.062	0.003	0.812	1
CRD vs P-CL	1.067	0.018	0.022	0.006	0.932	10
CRD vs LIF	1.076	0.023	0.031	0.007	0.899	10
CRD vs P-CL	1.136	0.036	0.007	0.014	0.959	60
CRD vs LIF	1.069	0.057	0.085	0.019	0.895	60

The 10 s data is presented in Fig. 4. The information below is for the line $NO_{2(LED\text{-}CRD)} = (m \pm e_m) * ref + (b \pm e_b)$. The reference values are either P-CL or LIF measurements

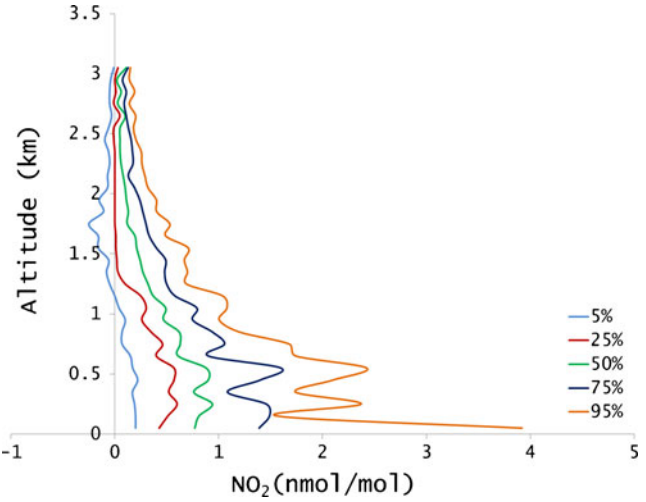

Fig. 5 Percentile analysis of 2011 flights, 6 June to 31 July. A total of 23 flights and 65 spirals, both AM and PM. BL measurements show more variability, but the variability smooths out with increasing altitude and distance from point sources

approximately 17 m above the water surface, spikes up to 14 and 17 nmol/mol NO_2 in air were observed. Between 1.3 and 2.1 km the degree of spatial homogeneity increases as NO_2 observations gradually slope negatively toward a low NO_x regime. Between 2.1 km and our maximum altitude, 3 km, NO_2 values are within bounds of a low NO_x regime. In the 2.1 to 3 km layer, the ozone production rate would be slow (Trainer et al. 1993; Kleinman et al. 1994), but cooler temperatures and greater wind speeds impact the lifetime and transport of NO_2 and NO_2 reaction products (i.e., ozone and particulate matter) contributing to wider ranging regional effects. Negative measurements, in the lowest percentile bin, are mostly in the LFT and are a reflection of the large standard deviation associated with measurements as atmospheric mixing ratios approach the instrument's detection limit. If the baseline of the cavity ringdown absorption monitor is stabilized, the improved signal to noise ratio at lower concentrations can result in a lower detection limit and the instrument may be suitable for measurements of NO_2 in more pristine environments. Measures to stabilize the optical cavity such as temperature control should be investigated.

4.4.2 Regional observations

Summer 2011 Maryland flight observations routinely show the presence of moderate levels of NO_2 in both upwind and downwind rural spiral locations. Figure 6 compares the median and quartile values of upwind and downwind column contents. The AM/Upwind profiles decrease exponentially with a scale height of≈1.2 km, while the PM/Downwind column distribution is fairly uniform up to 1.0 km, then gradually reaches the detection limit near 2.5 km. Figure 7 compares median NO_2 values for all DISCOVER-AQ observations in the Washington, D.C. / Baltimore metropolitan nonattainment area measured on both planes (all three instruments). Measurement sites are posted in Fig. 1. The P3 data show slightly higher levels of NO_2 in the BL near 0.4 km, than the downwind LED-CRD Cessna data due to the more urban flight P3 path. The P3 sampled five sites in the Baltimore nonattainment region and flew 47 low passes along the I-95 and 295. Between the different aircraft flight paths and spiral locations, the three

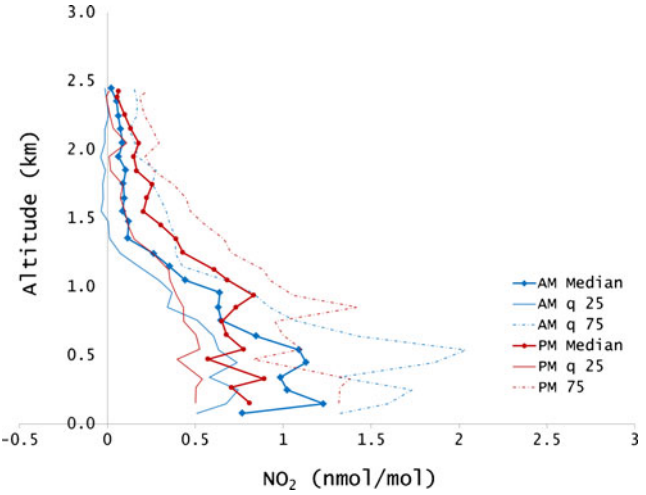

Fig. 6 AM/PM NO_2 quartiles. Comparison of NO_2 observations collected upwind and downwind of the Baltimore Washington metropolitan region. The *dotted lines* represent the median values which are bracketed by 25 % and 75 % quartiles. Upwind/AM measurements are before solar noon and downwind/PM measurements are after solar noon

combined NO_2 profiles show similar vertical columns for July, although BL measurements with more point source influence shows signs of a BL maximum between 0.4 and 0.5 km. The LED-CRD median PM profile over Maryland is similar to P-CL NO_2 observations made over the Donau Valley in Austria, May 2001, between altitudes of 0.9 km and 3 km (Heland et al. 2002). 82 % and 75 % of total NO_2 in the AM and PM columns, respectively, is observed to be below 1 km altitude. Similar BL/total column density ratios were observed in Houston, TX, 2004 and the Po Valley, Italy (2006) (Schaub et al. 2006; Ordó ez et al. 2006).

The sum of the binned UMD AM/Upwind column content was 2.97×10^{15} molecules/cm^2 and the sum of the binned UMD PM column content was 3.05×10^{15} molecules/cm^2. With 5 % measurement uncertainty, the averaged Baltimore/Washington, D.C. downwind vertical column content was not significantly different from the upwind column content indicating that

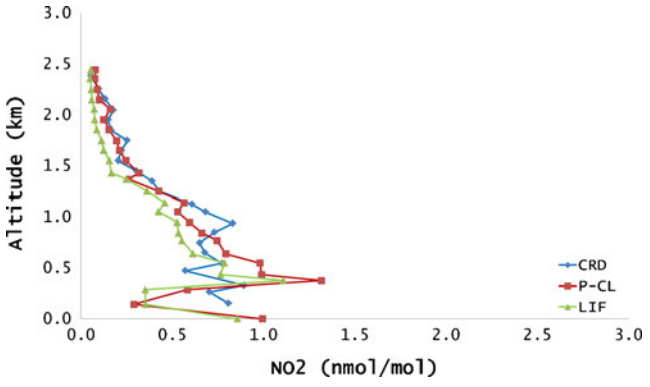

Fig. 7 A comparison of median CRD summertime aircraft measurements downwind of Baltimore to median P-CL and LIF measurements made along the Baltimore Washington urban corridor during DISCOVER AQ

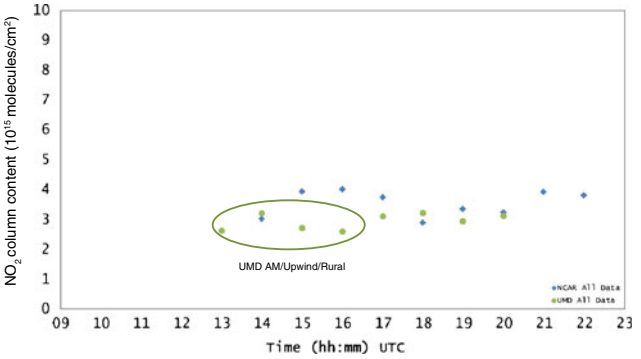

Fig. 8 Column content, hourly, from 1430 UTC to 2230 UTC. These are the NCAR P-CL and UMD CRD NO_2 measurements. The variation of the P3 NCAR hourly column content is 12 % while the variation of the UMD CRD column content is 32 %

changing near-surface measurements are influenced by BL dynamics. A Canadian study examining transport of polluted air across Lake St. Claire to rural Canada also observed, via Multi Axis Differential Optical Spectroscopy, that the integrated vertical column density showed less dependence on the time of day than did their BL measurements (Halla et al. 2011). Figure 8 shows the UMD regional column content binned by the hour in comparison to the P3 metropolitan area column content. The column contents shown here are limited to 0.3 km to 3.0 km, the altitude range covered by both planes. The hourly upwind column content is slightly (≈ 22 %) smaller than the measured column content for similar times in the metropolitan area. While there is more NO_2 measured over the urban area, upwind/rural NO_2 mixing ratios (for the same time of day) are substantial enough for ozone production in the BL, contributing to the regional nature of eastern U.S. air quality episodes (He et al. 2013a, b). The regionally averaged NO_2 vertical distribution with variations in the hourly resolution supports conclusions from Castellanos et al. (2011) indicating that model over estimations of urban NO_x and under estimation of rural NO_x is in part a result of too short NO_x lifetimes, and not accurately capturing advection between rural and urban areas.

5 Conclusion

This paper describes an updated, stabilized, commercially available cavity ringdown spectrometer that reliably measures ambient NO_2 at the surface and aloft. In an intercomparison with two well characterized NO_2 detectors, this instrument compared favorably for atmospheric NO_2 mixing ratios ranging from 0.08 nmol/mol and 1.3 nmol/mol in the BL and LFT.

The LED-CRD calibration coefficient was verified five times at three locations over 5 months via GPT and standard dilution. The sensitivity of the instrument was stable within 4 %.

Altitude profiles from 23 research flights (65 profiles) during the summer of 2011 were obtained upwind of the Baltimore/Washington, D.C. metropolitan area in the morning and downwind of the area in the afternoon. Looking at all observations collected during forecasted ozone events in the Mid- Atlantic States, the median (quartiles) NO_2 mixing ratio was 0.84 nmol/mol (0.5 nmol/mol to 1.4 nmol/mol) in the lowest 0.5 km and 0.21 nmol/mol (0.01 nmol/mol to 0.60 nmol/mol) nmol/mol at 1.5 km. More variability was observed in the BL.

Morning upwind NO_2 mixing ratios showed a rapid decrease between the BL and LFT with an effective scale height of ≈1.2 km in the morning. Afternoon downwind profiles were more

homogeneously distributed with a gradual decrease to the detection limit between 1.6 and 2.5 km. EKMA diagrams (e.g., Chameides et al. 1992) show that for the range of BL NO_2 mixing ratios observed here (0.5 nmol/mol to 1.5 nmol/mol) mid-day ozone production rates are relatively insensitive to volatile organic compound levels and range from 1 nmol/mol/h to 10 nmol/mol/h. Total column contents between the AM/upwind and PM/downwind were remarkably similar indicating that NO_2 is widely distributed over the eastern US contributing to the regional (spatial scales of approximately 1,000 km) nature of smog events.

Acknowledgments The aircraft flights were funded by Maryland Department of the Environment and the National Oceanic and Atmospheric Administration (NOAA). From NIST we thank Dave Duewer for help with data analysis and Jim Norris for calibrating the ozone monitor and primary standard. We thank Winston Luke, Paul Kelley and Xinrong Ren from the (NOAA) for conducting a month long field comparison to their P-CL NO_2 instrument. We thank Patricia Castellanos for instrument instruction and support. We thank NASA for supporting the DISCOVER-AQ air campaign and AURA and AQAST funding.

Disclaimer The identification of certain commercial equipment, instruments, or materials does not imply recommendation or endorsement by the National Institute of Standards and Technology. These identifications are made only in order to specify the experimental procedures in adequate detail.

References

Annesi-Maesano: Epidemiology of chronic obstructive pulmonary disease. In: Siafakas, N.M. (ed.) Management of chronic obstructive pulmonary disease, vol. 11, pp. 41–70. European Respiratory Society Journals Ltd, Wakefield (2006)

Blonde, N., Boersma, K.F., Eskes, H.J., van der A, R.J., Van Roozendael, M., De Smedt, I., Bergametti, G., Vautard, R.: Intercomparison of SCIAMACHY nitrogen dioxide observations, *In Situ* measurements and air quality modeling results over Western Europe. J. Geophys. Res. **112**, D10311 (2007). doi:10.1029/2006JD007277

Bucsela, E.J., Perring, A.E., Cohen, R.C., Boersma, K.F., Celarier, E.A., Gleason, J.F., Wenig, M.O., Bertram, T.H., Wooldridge, P.J., Dirksen, R., Veefkind, J.P.: Comparison of tropospheric NO_2 from In Situ aircraft measurements with near-real-time and standard product data from OMI. J. Geophys. Res. **113**, D16S31 (2008). doi:10.1029/2007JD008838

Busch, K.W., Busch, M.A.: Introduction to cavity-ringdown spectroscopy. In: Busch, K.W., Busch, M.A. (eds.) Cavity-Ringdown Spectroscopy. An Ultratrace-Absorption Measurement Technique, pp. 7–19. American Chemical Society, Washington, D.C (1999)

Castellanos, P., Luke, W.T., Kelley, P., Stehr, J.W., Ehrman, S.H., Dickerson, R.R.: Modification of a commercial cavity ring-down spectroscopy NO_2 detector for enhanced sensitivity. Rev. Sci. Instrum. **80**, 113107 (2009)

Castellanos, P., Marufu, L., Doddridge, B., Taubman, B., Schwab, J., Hains, J., Ehrman, S., Dickerson, R.: Ozone, oxides of nitrogen, and carbon monoxides during pollution events over the eastern United States: an evaluation of emissions and vertical mixing. J. Geophys. Res. **116**, D16307 (2011). doi:10.1029/2010JD014540

Chameides, W.L., Fehsenfeld, F., Rodgers, M.O., Cardelino, C., Martinez, J., Parrish, D., Lonneman, W., Lawson, D.R., Rasmussen, R.A., Zimmerman, P., Greenberg, J., Middleton, P., Wang, T.: Ozone precursor relationships in the ambient atmosphere. J. Geophys. Res. **97**(D5), 6037–6055 (1992)

Dari-Salisburgo, C., Di Carlo, P., Giammaria, G., Yoshizumi, K., D'Altorio, A.: Laser induced fluorescence instrument for NO_2 measurements: observations at a central Italy background site. Atmos. Environ. **43**, 970–977 (2009)

Day, D.A., Wooldridge, P.J., Dillon, M.B., Thornton, J.A., Cohen, R.C.: A thermal dissociation laser-induced fluorescence instrument for in situ detection of NO_2, peroxy nitrates, alkyl nitrates, and HNO_3. J. Geophys. Res. **207**(D6), 4046 (2002). doi:10.1029/2001JD000779

DiCarlo, P., Aruffo, E., Busilacchio, M., Glammaria, F., Dari-Salisburgo, C., Biancofiore, F., Visconti, G., Lee, J., Moller, S., Reeves, C.E., Bauguitte, S., Forster, G., Jones, R.L., Ouyang, B.: Aircraft based four-channel thermal dissociation laser induced fluorescence instrument for simultaneous measurements of NO_2, total peroxy nitrate, total alkyl nitrate, and HNO_3. Atmos. Meas. Tech. Discuss. **5**, 8759–8787 (2012)

Dunlea, E.J., Herndon, S.C., Nelson, D.D., Volkamer, R.M., San Martini, F., Sheehy, P.M., Zahniser, M.S., Shorter, J.H., Wormhoudt, J.C., Lamb, B.K., Allwine, E.J., Gaffney, J.S., Marley, N.A., Grutter, M.,

Marquez, C., Blanco, S., Cardenas, B., Retama, A., Ramos Villegas, C.R., Kolb, C.E., Molina, L.T., Molina, M.J.: Evaluation of nitrogen dioxide chemiluminescence monitors in a polluted urban environment. Atmos. Chem. Phys. Discuss. **7**, 569–604 (2007)

Emmons, L.K., Carroll, M.A., Hauglustaine, D.A., Brasseur, G.P., Atherton, C., Penner, J., Sillman, S., Levy II, H., Rohrer, F., Wauben, W.M.F., Van Velthoven, P.F.J., Wang, Y., Jacob, D., Bakwin, P., Dickerson, R., Doddridge, B., Gerbig, C., Honrath, R., Hübler, G., Jaffe, D., Kondo, Y., Munger, J.W., Torres, A., Volz-Thomas, A.: Climatologies of NO_x and NO_y: a comparison of data and models. Atmos. Environ. **31**(12), 1851–1904 (1997)

EPA: Report No. EPA/600/R-05/0004aA (2006)

Fehsenfeld, F.C., Dickerson, R.R., Hübler, G., Luke, W.T., Nunnermacker, L.J., Williams, E.J., Roberts, J.M., Calvert, J.G., Curran, C.M., Delany, A.C., Eubank, C.S., Fahey, D.W., Fried, A., Gandrud, B.W., Langford, A.O., Murphy, P.C., Norton, R.B., Pickering, K.E., Ridley, B.A.: A ground-based intercomparison of NO, NO_x, and NO_y measurement techniques. J. Geophys. Res. **92**(D12), 14710–14722 (1987)

Fehsenfeld, F.C., Williams, E.J., Buhr, M.P., Hubler, G., Langford, A.O., Murphy, P.C., Parish, D.D., Norton, R.B., Fahey, D.W., Drummond, J.W., Mackay, G.I., Roychowdhury, U.K., Hovermale, C., Mohnen, V.A., Demerjian, K.L., Galvin, P.J., Calvert, J.G., Ridley, B.A., Grahek, F., Heikes, B.G., Kok, G.L., Shetter, J.D., Walega, J.G., Elsworth, C.M., Schiff, H.I.: Intercomparison of NO_2 measurement techniques. J Geophys. Res. **95**(D4), (1990). doi:10.1029/JD095iD04p03579

Finlayson-Pitts, B.J., Pitts Jr., J.N.: Chemistry of the Upper and Lower Atmosphere: Theory, Experiments, and Applications. Academic, San Diego (2000). 4–8pp

Fried, A., Sams, R., Dorko, W., Elkins, J., Cai, Z.-T.: Determination of nitrogen dioxide in air compressed gas mixtures by quantitative tunable diode laser absorption spectrometry and chemiluminescence detection. Anal. Chem. **60**, 394–403 (1998)

Fuchs, H., Ball, S.M., Bohn, B., Brauers, T., Cohen, R.C., Dorn, H.-P., Dubé, W.P., Fry, J.L., Häseler, R., Heitmann, U., Jones, R.L., Kleffmann, J., Mentel, T.F., Müsgen, P., Rohrer, F., Rollins, A.W., Ruth, A.A., Kiendler-Scharr, A., Schlosser, E., Shillings, A.J.L., Tillmann, R., Varma, R.M., Venables, D.S., Villena Tapia, G., Wahner, A., Wegener, R., Wooldridge, P.J., Brown, S.S.: Intercomparison of measurements of NO_2 concentrations in the atmosphere simulation chamber SAPHIR during the NO3Comp campaign. Atmos. Meas. Tech. **3**, 21–37 (2010)

Halla, J.D., Wagner, T., Beirle, S., Brook, J.R., Hayden, K.L., O'Brien, J.M., Ng, A., Majonis, D., Wenig, M.O., McLaren, R.: Determination of tropospheric vertical columns of NO_2 and aerosol optical properties in a rural setting using MAX-DOAS. Atmos. Chem. Phys. **11**, 12475–12498 (2011)

Hargrove, J., Wang, L., Muyskens, K., Muyskens, M., Medina, D., Zaide, S., Zhang, J.: Cavity ring-down spectroscopy of ambient NO_2 with quantification and elimination of inteferences. Environ. Sci. Technol. **40**, 7868–7873 (2006)

He, H., Loughner, C., Stehr, J., Arkinson, H., Brent, L., Follette-Cook, M., Thompson, A., Diskin, G., Anderson, B., Crawford, J., Weinheimer, A., Cohen, R.C., Lee, P., Hains, J., Dickerson, R.: An elevated reservoir in a six-day pollution event over the Mid-Atlantic states: a case study from airborne measurements and numerical simulations. Atmos. Environ. (2013a)

He, H., Stehr, J., Hains, J., Krask, D., Doddridge, B., Vinnikov, K., Canty, T., Hosley, K., Salawitch, R., Worden, H., Dickerson, R.: Trends in emissions and concentrations of air pollutants in the lower troposphere in the Baltimore/Washington airshed from 1997 to 2011. Atmos. Chem. Phys. Discuss. **13**, 3135–3178 (2013b). doi:10.5194/acpd-13-3135-2013

Heland, J., Schlager, H.: First comparison of tropospheric NO_2 column densities retrieved from GOME measurements and *In Situ* aircraft profile measurments. Geophys. Res. Lett. **29**(20), (2002). doi:10.1029/2002GL015528

Herman, J., Cede, A., Spinei, E., Mount, G., Tzortziou, M., Abuhassan, N.: NO_2 column amounts from ground-based Pandora and MFDOAS spectrometers using the direct-sun DOAS technique: intercomparisons and application to OMI validation. J. Geophys. Res. **14**, D13307 (2009)

Jacob, D.J., Heikes, B.G., Fan, S.-M., Logan, J.A., Mauzerall, D.L., Bradshaw, J.D., Singh, H.B., Gregory, G.L., Talbot, R.W., Blake, D.R., Sachse, G.W.: Origin of ozone and NOx in the tropical troposphere: a photochemical analysis of aircraft observations over the South Atlantic basin. JGR **10**(D19), 24235–24250 (1996)

Jaeglé, L., Jacob, D.L., Wang, Y., Weinheimer, A.J., Ridley, B.A., Campos, T.L., Sachse, G.W., Hagen, D.E.: Sources and chemistry of NO_x in the upper troposphere over the United States. Geophys. Res. Lett. **25**(10), 1705–1708 (1998)

Kim, S.-W., Heckel, A., Frost, G.J., Richter, A., Gleason, J., Burrows, J.P., McKeen, S., Hsie, E.-Y., Cranier, C., Trainer, M.: NO_2 columns in the western United States observed from space and simulated by a regional chemistry model and their implications for NO_x emissions. J. Geophys. Res. **114**, D11301 (2009). doi:10.1029/2008JD011343

Kleinman, L.I., Lee, Y.-N., Springston, S.R., Nunnermacker, L., Zhou, X., Brown, R., Hallock, K., Klotz, P., Leahy, D., Lee, J.H., Newman, L.: Ozone formation at a rural site in the southeastern United States. J. Geophys. Res. **99**(D2), 3469–6482 (1994)

Lehmann, K., Berden, G., Engeln, R.: An introduction to cavity ring-down spectroscopy. In: Berden, G., Engeln, R. (eds.) Cavity Ring-Down Spectroscopy, pp. 6–10. Wiley, Chichester (2009)

Leue, C., Wenig, M., Wagner, T., Klimm, O., Platt, U., Jähne, B.: Quantitative analysis of NO_x emissions from Global Ozone Monitoring experiment satellite image sequences. J. Geophys. Res. **106**(D6), 5493–5505 (2001)

Logan, J.A.: Ozone in rural areas of the United States. J. Geophys. Res. **94**(D6), 8511–8532 (1989)

Luke, W.T., Dickerson, R.R., Ryan, W.F., Pickering, K.E., Nunnermacker, L.J.: Tropospheric chemistry over the lower great plains of the United States. 2. Trace gas profiles and distributions. J. Geophys. Res. **97**(D18), 20647–20670 (1992)

Luke, W.T., Arnold, J.R., Gunter, R.L., Watson, T.B., Wellman, D.L., Dasgupta, P.K., Li, J., Riemer, D., Tate, P.: The NOAA Twin Otter and its role in BRACE: platform description. Atmos. Environ. **41**, 4177–4189 (2007)

Napelenok, S.L., Pinder, R.W., Gilliland, A.B.., Martin, R.V.: A method for evaluating spatially-resolved NOx emissions using Kalman filter inversion, direct sensitivities, and space-based NO_2 observations. Atmos. Chem. Phys. **8**, 5603–5614 (2008)

Neuman, J.A., Gao, R.S., Fahey, D.W., Holecek, J.S., Ridley, B.A., Walega, J.G., Grahek, F.E., Richard, E.C., McElroy, C.T., Thompson, T.L., Elkins, J.W., Moore, F.L., Ray, E.A.: *In Situ* measurements of HNO_3, NO_y, NO and O3 in the lower stratosphere and upper troposphere. Atmos. Environ. **35**(33), 5789–5797 (2001)

Ordó ez, C., Tichter, A., Steinbacher, M., Zellweger, C., Nüss, H., Burrows, J.P., Pérvôt, A.S.H.: Comparison of 7 years of satellite-borne and ground-based tropospheric NO_2 measurements around Milan, Italy. J. Geophys. Res. **111**(D5), D05310 (2006). doi:10.1029/2005JD006305

Pollack, I.B., Lerner, B.M., Ryerson, T.B.: Evaluation of ultraviolet light-emitting diodes for detection of atmospheric NO_2 by photolysis-chemiluminescence. J. Atmos. Chem. **65**(2), 111–125 (2011)

Ryerson, T.B., Williams, E.J., Fehsenfeld, F.C.: An efficient photolysis system for fast-response NO2 measurements. JGR **105**(D21), 26,447–26,461 (2000)

Schaub, D., Boersma, K.F., Kaiser, J.W., Weiss, A.K., Folini, D., Eskes, H.J., Buchmann, B.: Comparison of GOME tropospheric NO_2 columns with NO_2 profiles deduced from ground-based *In Situ* measurements. J. Atmos. Chem. Phys. **6**, 3211–3229 (2006)

Schwartz, J., Zeger, S.: Passive smoking, air pollution, and acute respiratory symptoms in a diary study of student nurses. Am. J. Respir. Crit. Care Med. **1**(141), 62–67 (1990)

Skoog, D.A., Holer, F.J., Nieman, T.A.: Principles of Instrumental Analysis. Thomas Learning, Inc, Toronto (1998)

Suzuki, H., Miyao, Y., Nakayama, T., Pearce, J.K., Matsumi, Y., Takahashi, K., Kita, K., Tonokura, K.: Comparison of laser-induced fluorescence and chemiluminescence measurements of NO_2 at an urban site. Atmos. Environ. **45**, 6233–6240 (2011)

Thorn, W. J.: Preparation and Analysis of NO and NO_2 Gas Standard Reference Materials In Aluminum Cylinders, hh; Poster with Extended Abstract #2010-A-900-AWMA; presented at A&WMA's 103rd Annual Conference & Exhibition June 23, Calgary, Alberta, Canada (2010)

Thornton, J.A., Wooldridge, P.J., Cohen, R.C.: Atmospheric NO_2: *In Situ* laser- induced fluorescence detection at parts per trillion mixing ratios. Anal. Chem. **72**, 528 (2000)

Trainer, M., Parish, D.D., Buhr, M.P., Norton, R.B., Fehsenfeld, R.C., Anlauf, K.G., Bottenheim, J.W., Tang, Y.Z., Wiebe, H.A., Roberts, J.M., Tanner, R.L., Newman, L., Bowersox, V.C., Meagher, J.F., Olszyna, K.J., Rodgers, M.O., Wang, T., Berresheim, H., Demerjian, K.L., Roychowdhury, U.K.: Correlation of ozone with NO_y in photochemically aged air. J. Geophys. Res. **98**, 2917–2925 (1993)

United States Environmental Protection Agency, Office of Air and Radiation, Sources of Bias in the Gas Analyzer. In An Operator's guide to eliminating bias in CEM systems, United States Environmental Protection Agency. http://www.epa.gov/airmarkets/emissions/bias.html (1994).

Wagner, N., Dubé, W., Washenfelder, R., Young, C., Pollack, I., Ryerson, T., Brown, S.: Diode laser-based cavity ring-down instrument for NO_3, N_2O_5, NO, NO_2 and O_3 from aircraft. Atmos. Meas. Tech. **4**, 1227–1240 (2011). doi:10.5194/amt-4-1227-2011

Wooldridge, P.J., Perring, A.E., Bertram, T.H., Flocke, F.M., Roberts, J.M., Singh, H.B., Huey, L.G., Thornton, J.A., Wolfe, G.M., Murphy, J.G., Fry, J.L., Rollins, A.W., LaFranchi, B.W., Cohen, R.C.: Total peroxy nitrates (ΣPNs) in the atmosphere: the thermal dissociation –laser induced fluorescence (TD-LIF) technique and comparisons to speciated PAN measurements. Atmos. Meas. Tech. **3**, 593–607 (2010)